Rapid Communications

Why the critical temperature of high-T_c cuprate superconductors is so low: The importance of the dynamical vertex structure

Motoharu Kitatani,[1,2] Thomas Schäfer,[1,3,4] Hideo Aoki,[2,5] and Karsten Held[1]

[1]*Institute of Solid State Physics, Vienna University of Technology, A-1040 Vienna, Austria*

[2]*Department of Physics, University of Tokyo, Hongo, Tokyo 113-0033, Japan*

[3]*Collège de France, 11 place Marcelin Berthelot, 75005 Paris, France*

[4]*Centre de Physique Théorique, École Polytechnique, CNRS, route de Saclay, 91128 Palaiseau, France*

[5]*Electronics and Photonics Research Institute, Advanced Industrial Science and Technology (AIST), Tsukuba, Ibaraki 305-8568, Japan*

(Received 24 January 2018; revised manuscript received 14 December 2018; published 22 January 2019)

To fathom the mechanism of high-temperature (T_c) superconductivity, the dynamical vertex approximation is evoked for the two-dimensional repulsive Hubbard model. After showing that our results reproduce well the cuprate phase diagram with a reasonable T_c and dome structure, we keep track of the scattering processes that primarily affect T_c. We find that local *particle-particle* diagrams significantly screen the bare interaction at low frequencies, which in turn suppresses antiferromagnetic spin fluctuations and hence the pairing interaction. Thus we identify dynamical vertex corrections as one of the main oppressors of T_c, which may provide a hint toward higher T_c's.

DOI: 10.1103/PhysRevB.99.041115

I. INTRODUCTION

More than three decades after the discovery of high-T_c cuprate superconductors [1], the quest for higher (or even room-temperature) T_c superconductors remains one of the biggest challenges in solid-state physics. Despite intensive efforts, we are still stuck with $T_c \lesssim 130$ K [2]. Nonetheless the cuprates do remain arguably the most promising material class, at least at ambient pressure [3].

In this arena, theoretical estimations of T_c, specifically identifying the reason why it is so low (as compared with the starting electronic energy scales of ∼eV), should be imperative if one wants to possibly enhance T_c. Through many theories proposed and intensively debated, it has become clear that superconductivity in the cuprates is interlinked with electronic correlations, which are considered to mediate the pairing through spin fluctuations [4]. The simplest and most widely used model for cuprates is the repulsive Hubbard model on a square lattice, where a formidable problem is that the scale of T_c is orders of magnitude smaller than the Hubbard interaction U and the hopping amplitude t, which has been a key question from the early stage of high-T_c studies [5]. Various approaches have been employed to attack the problem; see, e.g., Refs. [6–13]. Thus, while the conventional phonon-mediated superconductors can now be accurately captured by density functional theory for superconductors (SCDFT) [14,15], a full understanding of T_c in the Hubbard model has yet to be achieved. One inherent reason for the low T_c is the d-wave symmetry of the gap function arising from the local repulsion.

A possibly essential mechanism that reduces T_c comes from vertex corrections. Migdal's theorem [16], which works so nicely for phonon-mediated pairing, is no longer applicable to unconventional superconductivity due to the electron correlation. For strongly correlated systems, we should in fact expect vertex corrections to be a major player, affecting T_c and changing it with respect to simpler (e.g., mean-field-like) treatments [17,18].

Thanks to recent extensions of the dynamical mean-field theory (DMFT) [19–21], specifically the dynamical vertex approximation (DΓA) [22–25], the dual-fermion [26], and other related approaches [13,27–32], such vertex corrections can now be studied for strong correlations; see [33] for a review. Due to this development, we now understand the (local) vertex structures much better [33–36], e.g., how they affect the spectral function and lead to pseudogaps in the normal phase [25,28,29,37–42]. This now puts us in a position to shed light on the impact of dynamical vertex corrections on superconductivity.

In this paper, we analyze how vertex corrections affect T_c. We find that the dynamical structure (frequency dependence) of the vertex, $\Gamma(\nu, \nu', \omega)$, is actually essential for estimating T_c. Note that Γ is nonperturbative; it sums up the local contribution of all Feynman diagrams (to all orders in the interaction) connecting two incoming and two outgoing particles. Physics of strongly correlated electrons such as the quasiparticle renormalization and the formation of Hubbard bands are hence encoded in Γ. On top of such correlations already included in DMFT, the DΓA further incorporates nonlocal correlations, in particular spin and superconducting fluctuations; see Fig. 1 and [33]. The present results show that the dynamics of Γ, which turns out to reduce the pairing interaction in a low-frequency regime, suppresses T_c by one order of magnitude. We unravel the physical origin in the relevant dynamical vertex structure as it is passed from the local vertex to the magnetic vertex describing antiferromagnetic spin fluctuations and, eventually, to the pairing interaction.

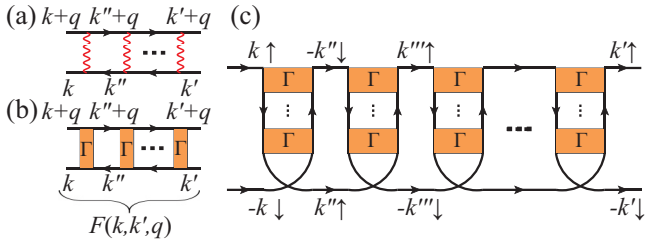

FIG. 1. (a) Antiferromagnetic spin fluctuations captured for weak interaction U (wiggled line) in terms of particle-hole ladder diagrams (solid line: Green's function). (b) DΓA diagrams describe similar spin fluctuations but now for strong correlation, with ladders in terms of the local Γ, which is nonperturbative and frequency-dependent [33] instead of U. (c) The spin fluctuations can act, in turn, as a pairing glue for superconductivity in the particle-particle channel (an exemplary diagram is shown).

II. MODEL AND METHODS

We consider the two-dimensional single-orbital Hubbard model,

$$\mathcal{H} = \sum_{\boldsymbol{k},\sigma} \epsilon(\boldsymbol{k}) c^{\dagger}_{\boldsymbol{k},\sigma} c_{\boldsymbol{k},\sigma} + U \sum_{i} \hat{n}_{i\uparrow}\hat{n}_{i\downarrow}, \tag{1}$$

where $c^{\dagger}_{\boldsymbol{k},\sigma}$ ($c_{\boldsymbol{k},\sigma}$) creates (annihilates) an electron with spin $\sigma = \uparrow, \downarrow$ and wave vector $\boldsymbol{k}$, U is the on-site Coulomb repulsion, and $\hat{n}_{i\sigma} \equiv c^{\dagger}_{i\sigma} c_{i\sigma}$. The two-dimensional band dispersion is given by $\epsilon(\boldsymbol{k}) = -2t(\cos k_x + \cos k_y) - 4t' \cos k_x \cos k_y - 2t''(\cos 2k_x + \cos 2k_y)$, with t, t', and t'' being the nearest-, second-, and third-neighbor hoppings, respectively. We consider two sets of hopping parameters: (a) $t' = t'' = 0$ and (b) $t'/t = -0.20$, $t''/t = 0.16$, which corresponds to the band structure of $HgBa_2CuO_{4+\delta}$ [43,44].

We adopt the DΓA as a method that incorporates nonlocal correlations beyond the local correlations treated in DMFT. In the DΓA [22,25,33], the local two-particle vertex Γ that is irreducible in the particle-hole channel is calculated from a DMFT impurity problem. We employ the exact diagonalization as an impurity solver to this end, but we also checked against quantum Monte Carlo simulations [45–48]; see the Supplemental Material [49].

From $\Gamma_{\sigma\sigma'}(\nu, \nu', \omega)$, the nonlocal vertex $F_{\sigma\sigma'}(k, k', q)$, which describes, among other things, longitudinal and transversal spin-fluctuations, is obtained via the Bethe-Salpeter equation in the vertical particle-hole channel [as visualized in Fig. 1(b)] and transversal particle-hole channel (not shown). $F_{\sigma\sigma'}(k, k', q)$ depends on the spin (σ, σ'), two fermionic (k, k'), and one bosonic (q) four-vectors consisting of momentum and Matsubara frequency, i.e., $k = (\boldsymbol{k}, \nu)$. From F, the DΓA self-energy $\Sigma(k)$ is in turn computed via the Schwinger-Dyson equation [33]; spin fluctuations included in $\Sigma(k)$ give rise to a pseudogap in the nonlocal Green's function $G(k)$ [25,39,49].

For studying superconductivity, we extend here the existing DΓA treatment. That is, we extract, from F, the particle-particle irreducible vertex $\Gamma_{\rm pp}(k, k', q = 0) \equiv F(k', -k, k - k') - \Phi_{\rm pp}(\nu, \nu', \omega = 0)$ (with four-vector in particle-particle convention). Here $\Phi_{\rm pp}$ is defined as the *local* reducible vertex diagrams in the particle-particle channel, which are included in F but need to be subtracted to obtain the $\Gamma_{{\rm pp},\,\boldsymbol{Q}=\boldsymbol{k}-\boldsymbol{k}'}(\nu, \nu')$, see [49] for details. The vertex $\Gamma_{\rm pp}$ contains spin fluctuations as a pairing glue, and we can now insert it into the particle-particle ladder [as illustrated in Fig. 1(c) for selected diagrams]. For evaluating this ladder, we use the linearized gap (Eliashberg) equation [50]:

$$\lambda \Delta(k) = -\frac{1}{\beta N_{\boldsymbol{k}}} \sum_{k'} \Gamma_{\rm pp}(k, k', q = 0) G(k') G(-k') \Delta(k'). \tag{2}$$

Here, $\Delta(k)$ is the anomalous self-energy, λ is the superconducting eigenvalue with $\lambda \to 1$ signaling an instability toward superconductivity [51], $\beta = 1/T$ is the inverse temperature, and $N_{\boldsymbol{k}}$ is the number of $\boldsymbol{k}$ points.

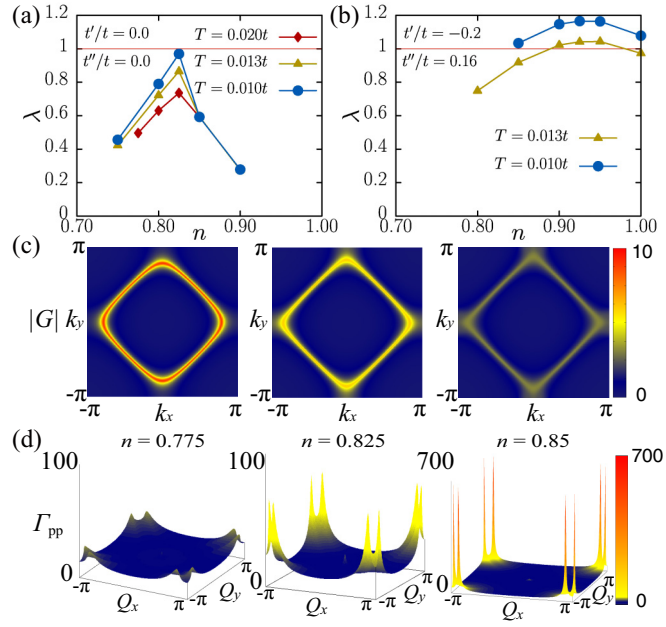

FIG. 2. d-wave eigenvalue λ against the band filling n for $U = 6t$, $T/t = 0.010, 0.013, 0.020$ with (a) $t' = t'' = 0$ and (b) $t'/t = -0.20$, $t''/t = 0.16$. (c,d) Momentum dependence of the Green's function $|G(\pi/\beta, \boldsymbol{k})|$ (c) and the pairing interaction vertex $\Gamma_{{\rm pp},\boldsymbol{Q}}$ (d) for $n = 0.775$ (overdoped), 0.825 (optimally doped), and 0.85 (underdoped), at $T/t = 0.02$ with other parameters as in (a). In (d) we specifically display the $\boldsymbol{Q}$ dependence of the pairing vertex $[\Gamma_{{\rm pp},\boldsymbol{Q}}(\pi/\beta, \pi/\beta) + \Gamma_{{\rm pp},\boldsymbol{Q}}(-\pi/\beta, \pi/\beta)]/2$, which is symmetrized for d-wave (singlet, even-frequency) pairing.

III. SIZE AND DOME SHAPE OF T_c

We first show the superconducting eigenvalue λ for the two sets of hopping parameters in Figs. 2(a) and 2(b), respectively. In the doping region in Fig. 2, the d-wave has the largest λ, while antiferromagnetic fluctuations become dominant close to half-filling; cf. Refs. [25,52]. A superconducting instability ($\lambda \to 1$) is found for $T_c \lesssim 0.01t$ in Fig. 2(a) and for $T_c \approx 0.015t$ in Fig. 2(b).

The results reproduce well the phase diagram of the cuprates with a dome structure and peaks that amount to $T_c \approx 50$–80 K around $n = 0.80$–0.95 if we take a typical $t \approx 0.45$ eV [53]. We can explain the physical origin of the

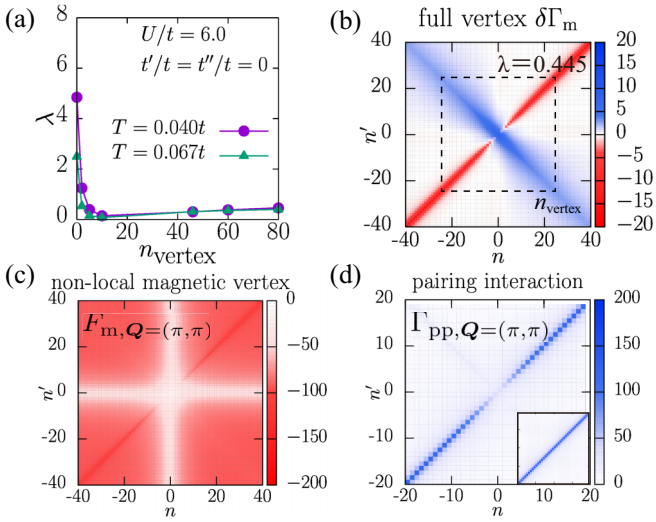

FIG. 3. (a) Eigenvalue λ against the frequency range $n_{\rm vertex}$ [exemplified in (b) as a dashed line], over which the local vertex correction $\delta\Gamma_{\rm m}$ is considered, for $U = 6t$, $t' = t'' = 0$, $n = 0.825$, and $T/t = 0.040, 0.067$. (b,c,d) Dynamical vertex structure of (b) the local vertex correction $\delta\Gamma_{\rm m}(\nu_n, \nu_{n'}, \omega = 0)$ in the magnetic channel relative to $-U$, (c) the nonlocal vertex in the magnetic channel, $F_{{\rm m},\boldsymbol{Q}=(\pi,\pi)}(\nu_n, \nu_{n'}, \omega = 0)$, and (d) the pairing interaction $\Gamma_{{\rm pp},\boldsymbol{Q}=(\pi,\pi)}(\nu_n, \nu_{n'}, \omega = 0)$, for the same U, t', t'', n with $T/t = 0.067$ here. The inset in (d) shows a typical structure of $\Gamma_{\rm pp}$ in mean-field-like approaches.

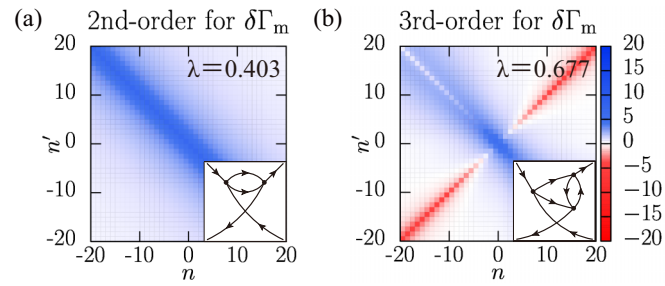

FIG. 4. Frequency structure of the local vertex correction, $\delta\Gamma_{\rm m}(\nu_n, \nu_{n'}, \omega = 0) \equiv \Gamma_{\rm m}(\nu_n, \nu_{n'}, \omega = 0) - (-U)$, for (a) second-order or (b) third-order perturbation theory for $U = 6t$, $t' = t'' = 0$, $n = 0.825$, and $T/t = 0.067$. In each panel, the inset shows a typical diagram taken into account, and the corresponding eigenvalue λ is indicated.

T_c dome as follows: antiferromagnetic spin fluctuations that mediate the pairing become stronger [i.e., $\Gamma_{\rm pp}$ in Fig. 2(d) increases] toward half-filling, while close to half-filling the self-energy blows up and damps $|G(k)|$ in Fig. 2(c). The latter eventually leads to a pseudogap at smaller dopings within the central peak in a three-peak spectrum; see the Supplemental Material [49]. Thus the dome appears as a consequence of two opposing factors: $\Gamma_{\rm pp}$ and $G(k)$ in the gap equation (2). We can see in Fig. 2(d) that $\Gamma_{\rm pp}$ is sharply peaked at around $\boldsymbol{Q} = (\pm\pi, \pm\pi)$ (with some offset and splitting because of incommensurability), leading to a d-wave $\Delta(k)$ in Eq. (2). Let us note that a superconducting dome has also been reported in, e.g., [6,7,12,13], but not in the dual-fermion approach [9,11].

IV. IMPORTANCE OF THE DYNAMICAL VERTEX STRUCTURE

Let us now look into the structure of the vertex $\Gamma(\nu, \nu', \omega = 0)$ against frequencies ν, ν'. As we shall see below, if we start from a mean-field or random phase approximation (RPA)-like treatment, where $\Gamma_{\rm m}(\nu, \nu', \omega) = \Gamma_{\uparrow\uparrow} - \Gamma_{\uparrow\downarrow}$ is replaced with the bare $-U$ in the Bethe-Salpeter ladder [54], this would yield stronger spin fluctuations and overestimate T_c by an order of magnitude.

We can elucidate this point in an energy-resolved fashion by taking the local irreducible vertex in the magnetic channel $\Gamma_{\rm m}(\nu, \nu', \omega)$ only up to a frequency $n_{\rm vertex}$, with the bare $(-U)$ adopted outside this range [55] [pictorially this means taking Fig. 1(a) instead of Fig. 1(b) for large frequencies]. In Fig. 3(a), we plot the eigenvalue λ against $n_{\rm vertex}$ [56]. As the region $n_{\rm vertex}$ in which we take the dynamical vertex is widened, λ is seen to dramatically decrease, already when a few frequencies are taken into account. This signifies that the *low-frequency part* of the dynamical $\Gamma_{\rm m}$ is quite important.

Figure 3(b) displays the deviation, $\delta\Gamma_{\rm m}(\nu_n, \nu_{n'}, \omega = 0) \equiv \Gamma_{\rm m}(\nu_n, \nu_{n'}, \omega = 0) - (-U)$, of the local Γ_m from $-U$. $\Gamma_{\rm m}$ is indeed prominently reduced (dark blue $\delta\Gamma_{\rm m}$) at small frequencies $\nu_n, \nu_{n'} \sim 0$, as well as along the diagonal $\nu_n = -\nu_{n'}$.

The nonlocal magnetic vertex $F_{\rm m}$ [Fig. 3(c)] and the pairing interaction $\Gamma_{\rm pp}$ [Fig. 3(d)] inherit similar dynamical structures from the local $\Gamma_{\rm m}$. This comes from the Bethe-Salpeter equation $F_{\rm m} = \Gamma_{\rm m} - \Gamma_{\rm m}\chi_0 F_{\rm m}$ with χ_0 being the bare bubble susceptibility, and from $\Gamma_{\rm pp} = F - \Phi_{\rm pp}$, respectively; for a more extensive discussion, see the Supplemental Material [49]. Without the vertex $\delta\Gamma_{\rm m}$, $F_{\rm m}$ depends on the spin susceptibility through $F_{\rm m} = -U - U^2\chi_{\rm m}(\omega)$ [49] and hence only on ω, which corresponds to the red background in Fig. 3(c). As a consequence, the pairing vertex $\Gamma_{\rm pp}$ depends only on the difference of two frequencies $\nu_n, \nu_{n'}$ [inset of Fig. 3(d)]. With the suppressed $\Gamma_{\rm pp}$, the Eliashberg Eq. (2) finally leads to a reduced λ and T_c. Thus we have traced that the local vertex corrections are responsible for the reduction of T_c, where an important message is that their *dynamical* structure has to be examined. Indeed, a mean-field-like (e.g., paramagnon-exchange) picture cannot describe the frequency structure in Fig. 3(d) even if we consider vertex correction effects on the susceptibility $\chi_{\rm m}(\omega)$.

V. PHYSICS BEHIND SUPPRESSION OF $\Gamma_{\rm m}$

Having identified the suppression of the local $\Gamma_{\rm m}$ as the key ingredient for low T_c's, we can now pinpoint which physical processes are at its origin. In Fig. 4 we show the contributions to $\delta\Gamma_{\rm m}$ in (a) second-order and (b) third-order perturbation theory, where we show a typical diagram along with the eigenvalue λ estimated in DΓA when $\Gamma_{\rm m}$ is replaced by the displayed local vertex [56]. When the bare value $(-U; \delta\Gamma_{\rm m} = 0)$ is used instead of the full $\Gamma_{\rm m}$, λ is enhanced dramatically from the correct value 0.45 to 2.49 for $T/t = 0.067$ (T_c increases correspondingly from $0.01t$ to $0.13t$). We can see that most of the dynamical effect is already included in the second-order particle-particle diagram in Fig. 4(a), which compensates the bare contribution $(-U)$ for $\nu_n \approx -\nu_{n'}$, and

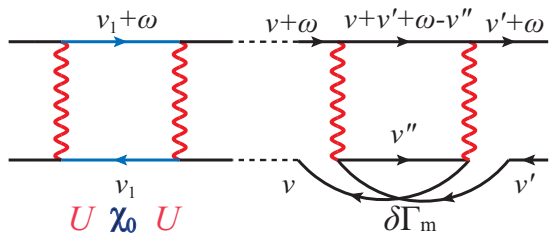

FIG. 5. Typical diagrams that contribute to the magnetic vertex F_m in the Bethe-Salpeter ladder. Left: a typical diagram as in RPA with U (red wavy line) as an irreducible building block, connected by χ_0 (with two Green's functions having fermionic frequencies ν_1 and $\nu_1+\omega$). Right: local (second-order) vertex correction $\delta\Gamma_m$ with a *particle-particle* bubble. Such terms are particle-hole irreducible, hence they need to be inserted in the Bethe-Salpeter ladder for spin fluctuations. They lead to the suppression of Γ_m in Fig. 4, and through the whole ladder suppress F_m and Γ_{pp} in Figs. 3(c) and 3(d).

strongly reduces λ back to 0.40. Third-order diagrams in Fig. 4(b) slightly enhance λ, and already resemble the full vertex qualitatively. Thus the second-order particle-particle diagrams in Fig. 4(a) constitute by far the major process for the suppression of the λ.

Hence it is worthwhile to look into this second-order contribution in more detail. The local irreducible vertex Γ_m is the building block for the nonlocal particle-hole ladder that leads to magnetic fluctuations as visualized in Fig. 1(b). If we take $\Gamma_m(\nu,\nu',\omega)=-U$ as in Fig. 1(a) or the left part of Fig. 5, we obtain the standard RPA with a Stoner-enhanced spin susceptibility,

$$\chi=\chi_0/(1-U\chi_0)=\chi_0+\chi_0U\chi_0+\chi_0U\chi_0U\chi_0\cdots. \quad (3)$$

While all the terms enhance the susceptibility in this geometric series in U, local vertex corrections do need to be included in the particle-hole ladder with $\Gamma_m(\nu,\nu',\omega)=-U+\delta\Gamma_m(\nu,\nu',\omega)$ as a building block. In Fig. 4(a), we have identified the second-order particle-particle contribution to $\delta\Gamma_m>0$ to be most important for suppressing antiferromagnetic spin fluctuations, and the inclusion of such a contribution $\delta\Gamma_m$ in the ladder series for F_m is visualized in the right part of Fig. 5.

The difference from the RPA ladder comprising $-U$ and *particle-hole* bubbles (left block in Fig. 5) is that $\delta\Gamma_m>0$ has (in the second order) two $-U$'s and a local *particle-particle* bubble (right block in Fig. 5). This bubble, being a particle-particle bubble, depends on the frequency combination $\nu+\nu'+\omega$ rather than on ω alone as in particle-hole bubbles. This, first of all, gives the pronounced frequency structure of $\delta\Gamma_m$ in Fig. 4(a). Since Fig. 5 shows typical diagrams that contribute to F_m, we can also see that, with a $\delta\Gamma_m$ located at an end of the ladder, F_m and $\Gamma_{pp}=F-\Phi_{pp}$ inherit a similar frequency structure as in Figs. 3(c) and 3(d); see the Supplemental Material [49] for a general explanation.

Second, at its maximum ($\omega=0,\nu'=-\nu$), the particle-particle bubble $\sum_{\nu''}G(\nu'')G(-\nu'')=\sum_{\nu''}G(\nu'')G^*(\nu'')$ has a sign opposite to the particle-hole bubble $\sum_{\nu''}G(\nu'')G(\nu'')$, because the biggest contribution comes from $\mathrm{Im}\,G(\nu)$. Hence $\delta\Gamma_m$ partially compensates the second-order RPA contribution, $U\chi_0U$ in Eq. (3). This is the reason why $\delta\Gamma_m$ reduces the bare U, whereas the RPA ladders Eq. (3) enhance it.

Now we are in a position to finally grasp a physical picture: while a repulsive interaction can give rise to a spin-fluctuation mediated attraction through the particle-hole channel, a local repulsive interaction U always leads to a repulsion between two particles in the particle-particle channel, too. As we have seen in Fig. 5, this repulsion in the particle-particle channel reduces the antiferromagnetic spin fluctuations, albeit only for certain frequency combinations. With reduced antiferromagnetic spin fluctuations, superconductivity is suppressed.

VI. CONCLUSION AND OUTLOOK

We have extended the DΓA formalism for studying superconductivity in the repulsive Hubbard model on a square lattice. Our results reproduce well the superconducting dome and typical values of $T_c\approx 50$–80 K for the cuprates. We have pinpointed the importance of dynamical vertex corrections. That is, T_c would be around room temperature if the pairing interaction was built from a ladder with the bare interaction U. However, local vertex corrections give rise to a pronounced frequency structure accompanied by a suppression (screening) of the irreducible magnetic vertex Γ_m (i.e., the effective interaction in the magnetic channel). This in turn suppresses antiferromagnetic spin fluctuations and the pairing glue (Γ_{pp}) for superconductivity in the particle-particle channel.

Thus local particle-particle fluctuations are at the origin of the suppression of Γ_m, so that it is intriguing to ask: can one possibly evade this oppressor of T_c? This is not simple. As the leading correction that reduces the bare interaction U is $\sim U^2$, the suppression becomes smaller for weaker Coulomb interactions, but so do the antiferromagnetic spin fluctuations. Local particle-particle fluctuations can be suppressed by disorder or a magnetic field [57], but this would degrade the nonlocal particle-particle (superconducting) fluctuations, too. One way out might be to exploit the characteristic frequency structure of Γ_m, possibly in combination with a frequency-dependent (local) interaction, which may originate from off-site (extended Hubbard) interactions as described in dual-boson [58] and extended-DMFT [59–63] approaches, or from phonons. A further route may be a proper design of the band structure, including multiorbital models. Another, completely different outcome of the frequency structure in the vertex is that it may possibly realize exotic gap functions on the frequency axis.

ACKNOWLEDGMENTS

We thank P. Gunacker for providing quantum Monte Carlo results for comparison for the vertex and self-energy. We benefited from illuminating discussions with A. Toschi, G. Rohringer, and P. Thunström. The present work was supported by European Research Council under the European Union's Seventh Framework Program (FP/2007-2013) through ERC Grant No. 306447, SFB ViCoM (M.K.,T.S.,K.H.), Austrian Science Fund (FWF) through the Doctoral School "Building Solids for Function" (T.S.), and the Erwin-Schrödinger Fellowship J 4266 (SuMo, T.S.), as well as by JSPS KAKENHI Grant No. JP26247057 and ImPACT Program of Council for

Science, Technology and Innovation, Cabinet Office, Government of Japan (Grant No. 2015-PM12-05-01) (M.K.,H.A.). T.S. also acknowledges the European Research Council for the European Union Seventh Framework Program (FP7/2007-2013) with ERC Grant No. 319286 (QMAC). H.A. wishes to thank the Department of Physics, ETH Zürich, Switzerland, for hospitality. Calculations have been done mainly on the Vienna Scientific Cluster (VSC).

[1] J. G. Bednorz and K. A. Müller, Z. Phys. B: Condens. Matter **64**, 189 (1986).
[2] A. Schilling, M. Cantoni, J. D. Guo, and H. R. Ott, Nature (London) **363**, 56 (1993).
[3] A. P. Drozdov, M. I. Eremets, I. A. Troyan, V. Ksenofontov, and S. I. Shylin, Nature (London) **525**, 73 (2015).
[4] D. J. Scalapino, Rev. Mod. Phys. **84**, 1383 (2012).
[5] P. A. Lee and N. Read, Phys. Rev. Lett. **58**, 2691 (1987).
[6] B. Kyung, J.-S. Landry, and A.-M. S. Tremblay, Phys. Rev. B **68**, 174502 (2003).
[7] T. Maier, M. Jarrell, T. Pruschke, and M. H. Hettler, Rev. Mod. Phys. **77**, 1027 (2005); S. Sakai, M. Civelli, and M. Imada, Phys. Rev. Lett. **116**, 057003 (2016).
[8] P. A. Lee, N. Nagaosa, and X.-G. Wen, Rev. Mod. Phys. **78**, 17 (2006).
[9] H. Hafermann, M. Kecker, S. Brener, A. N. Rubtsov, M. I. Katsnelson, and A. I. Lichtenstein, J. Supercond. Nov. Magn. **22**, 45 (2009).
[10] W. Metzner, M. Salmhofer, C. Honerkamp, V. Meden, and K. Schönhammer, Rev. Mod. Phys. **84**, 299 (2012).
[11] J. Otsuki, H. Hafermann, and A. I. Lichtenstein, Phys. Rev. B **90**, 235132 (2014).
[12] M. Kitatani, N. Tsuji, and H. Aoki, Phys. Rev. B **92**, 085104 (2015).
[13] J. Vučičević, T. Ayral, and O. Parcollet, Phys. Rev. B **96**, 104504 (2017).
[14] M. Lüders, M. A. L. Marques, N. N. Lathiotakis, A. Floris, G. Profeta, L. Fast, A. Continenza, S. Massidda, and E. K. U. Gross, Phys. Rev. B **72**, 024545 (2005).
[15] M. A. L. Marques, M. Lüders, N. N. Lathiotakis, G. Profeta, A. Floris, L. Fast, A. Continenza, E. K. U. Gross, and S. Massidda, Phys. Rev. B **72**, 024546 (2005).
[16] A. B. Migdal, Sov. Phys. JETP **7**, 996 (1958).
[17] S. Onari, Y. Yamakawa, and H. Kontani, Phys. Rev. Lett. **112**, 187001 (2014).
[18] D. Vilardi, C. Taranto, and W. Metzner, Phys. Rev. B **96**, 235110 (2017).
[19] W. Metzner and D. Vollhardt, Phys. Rev. Lett. **62**, 324 (1989).
[20] A. Georges and G. Kotliar, Phys. Rev. B **45**, 6479 (1992).
[21] A. Georges, G. Kotliar, W. Krauth, and M. J. Rozenberg, Rev. Mod. Phys. **68**, 13 (1996).
[22] A. Toschi, A. A. Katanin, and K. Held, Phys Rev. B **75**, 045118 (2007).
[23] H. Kusunose, J. Phys. Soc. Jpn. **75**, 054713 (2006).
[24] C. Slezak, M. Jarrell, T. Maier, and J. Deisz, J. Phys.: Condens. Matter **21**, 435604 (2009).
[25] A. A. Katanin, A. Toschi, and K. Held, Phys. Rev. B **80**, 075104 (2009).
[26] A. N. Rubtsov, M. I. Katsnelson, and A. I. Lichtenstein, Phys. Rev. B **77**, 033101 (2008).
[27] G. Rohringer, A. Toschi, H. Hafermann, K. Held, V. I. Anisimov, and A. A. Katanin, Phys. Rev. B **88**, 115112 (2013).
[28] C. Taranto, S. Andergassen, J. Bauer, K. Held, A. Katanin, W. Metzner, G. Rohringer, and A. Toschi, Phys. Rev. Lett. **112**, 196402 (2014).
[29] T. Ayral and O. Parcollet, Phys Rev. B **92**, 115109 (2015).
[30] G. Li, Phys. Rev. B **91**, 165134 (2015).
[31] T. Ayral and O. Parcollet, Phys. Rev. B **93**, 235124 (2016).
[32] T. Ayral and O. Parcollet, Phys. Rev. B **94**, 075159 (2016).
[33] G. Rohringer, H. Hafermann, A. Toschi, A. A. Katanin, A. E. Antipov, M. I. Katsnelson, A. I. Lichtenstein, A. N. Rubtsov, and K. Held, Rev. Mod. Phys. **90**, 025003 (2018).
[34] G. Rohringer, A. Valli, and A. Toschi, Phys. Rev. B **86**, 125114 (2012).
[35] G. Rohringer, Ph.D. thesis, Vienna University of Technology, 2013.
[36] N. Wentzell, G. Li, A. Tagliavini, C. Taranto, G. Rohringer, K. Held, A. Toschi, and S. Andergassen, arXiv:1610.06520.
[37] A. N. Rubtsov, M. I. Katsnelson, A. I. Lichtenstein, and A. Georges, Phys. Rev. B **79**, 045133 (2009).
[38] T. Schäfer, F. Geles, D. Rost, G. Rohringer, E. Arrigoni, K. Held, N. Blümer, M. Aichhorn, and A. Toschi, Phys. Rev. B **91**, 125109 (2015).
[39] T. Schäfer, A. Toschi, and K. Held, J. Magn. Magn. Mater. **400**, 107 (2016).
[40] O. Gunnarsson, T. Schäfer, J. P. F. LeBlanc, E. Gull, J. Merino, G. Sangiovanni, G. Rohringer, and A. Toschi, Phys. Rev. Lett. **114**, 236402 (2015).
[41] P. Pudleiner, T. Schäfer, D. Rost, G. Li, K. Held, and N. Blümer, Phys. Rev. B **93**, 195134 (2016).
[42] O. Gunnarsson, J. Merino, T. Schäfer, G. Sangiovanni, G. Rohringer, and A. Toschi, Phys. Rev. B **97**, 125134 (2018).
[43] K. Nishiguchi, K. Kuroki, R. Arita, T. Oka, and H. Aoki, Phys. Rev. B **88**, 014509 (2013).
[44] K. Nishiguchi, Ph.D. thesis, University of Tokyo, 2012.
[45] P. Werner, A. Comanac, L. de'Medici, M. Troyer, and A. J. Millis, Phys. Rev. Lett. **97**, 076405 (2006).
[46] P. Werner and A. J. Millis, Phys. Rev. B **74**, 155107 (2006).
[47] N. Parragh, A. Toschi, K. Held, and G. Sangiovanni, Phys. Rev. B **86**, 155158 (2012).
[48] M. Wallerberger, A. Hausoel, P. Gunacker, A. Kowalski, N. Parragh, F. Goth, K. Held, and G. Sangiovanni, Comput. Phys. Commun. **235**, 388 (2019).
[49] See Supplemental Material at http://link.aps.org/supplemental/10.1103/PhysRevB.99.041115 for further details on the relation between Γ_m and F, including the λ-correction of the physical susceptibility (Sec. S.1), a demonstration of the convergence of the results with respect to the frequency box (Sec. S.2), a comparison with CT-QMC results for λ (Sec. S.3), and a demonstration of how a pseudogap develops in the present formalism (Sec. S.4).
[50] This is a first step toward the more involved parquet DΓA [33].
[51] Note that a quasi-two-dimensional (2D) system has a finite T_c if 2D layers are stacked and weakly interacting with each

other. For a genuinely 2D system, to which the Mermin-Wagner theorem applies, the feedback effect of the d-wave pairing fluctuations on the self-energy needs to be taken into account, as in, e.g., a parquet formalism [64–66].

[52] T. Schäfer, A. A. Katanin, K. Held, and A. Toschi, Phys. Rev. Lett. **119**, 046402 (2017).

[53] H. Sakakibara, H. Usui, K. Kuroki, R. Arita, and H. Aoki, Phys. Rev. Lett. **105**, 057003 (2010).

[54] Note that FLEX as supplemented by the local DMFT self-energy for the local part (FLEX+DMFT) also gives rather high T_c's [12].

[55] Namely, outside the frequency box $[(-2n_{\mathrm{vertex}}+1)\pi/\beta \leqslant \nu, \nu' \leqslant (2n_{\mathrm{vertex}}-1)\pi/\beta, (-2n_{\mathrm{vertex}}+2)\pi/\beta \leqslant \omega \leqslant (2n_{\mathrm{vertex}}-2)\pi/\beta]$.

[56] Note that we focus on the effect of the vertex structure in Eq. (2), and keep Green's functions fixed here, i.e., we always employ, *unlike* in RPA, Green's functions that incorporate the self-energy from the full Γ_{m}.

[57] B. L. Altshuler and A. G. Aronov, *Electron-Electron Interaction in Disordered Conductors*, edited by A. I. Efros and M. Pollak (Elsevier Science Publisher, Amsterdam, 1985).

[58] A. N. Rubtsov, M. I. Katsnelson, and A. I. Lichtenstein, Ann. Phys. **327**, 1320 (2012).

[59] A. M. Sengupta and A. Georges, Phys. Rev. B **52**, 10295 (1995).

[60] Q. Si and J. L. Smith, Phys. Rev. Lett. **77**, 3391 (1996).

[61] J. L. Smith and Q. Si, Phys. Rev. B **61**, 5184 (2000).

[62] R. Chitra and G. Kotliar, Phys. Rev. B **63**, 115110 (2001).

[63] P. Sun and G. Kotliar, Phys. Rev. B **66**, 085120 (2002).

[64] K.-M. Tam, H. Fotso, S.-X. Yang, T.-W. Lee, J. Moreno, J. Ramanujam, and M. Jarrell, Phys. Rev. E **87**, 013311 (2013).

[65] A. Valli, T. Schäfer, P. Thunström, G. Rohringer, S. Andergassen, G. Sangiovanni, K. Held, and A. Toschi, Phys. Rev. B **91**, 115115 (2015).

[66] G. Li, N. Wentzell, P. Pudleiner, P. Thunström, and K. Held, Phys. Rev. B **93**, 165103 (2016).